Proc. Natl. Acad. Sci. USA
Vol. 95, pp. 945–950, February 1998
Biochemistry

Structure of the elongating ribosome: Arrangement of the two tRNAs before and after translocation

(protein synthesis/neutron scattering/tRNA binding sites)

KNUD H. NIERHAUS*†, JÖRG WADZACK*, NILS BURKHARDT*‡, RALF JÜNEMANN*, WOLF MEERWINCK‡, REGINE WILLUMEIT‡, AND HEINRICH B. STUHRMANN‡

*MPI für Molekulare Genetik, AG Ribosomen, Ihnestrasse 73, D-14195 Berlin, Germany; and ‡Forschungszentrum GKSS, Max-Planck-Strasse, D-21502 Geesthacht, Germany

Communicated by Hans Frauenfelder, Los Alamos National Laboratory, Los Alamos, NM, November 26, 1997 (received for review March 10, 1997)

ABSTRACT **The ribosome uses tRNAs to translate the genetic information into the amino acid sequence of proteins. The mass ratio of a tRNA to the ribosome is in the order of 1:100; because of this unfavorable value it was not possible until now to determine the location of tRNAs within the ribosome by neutron-scattering techniques. However, the new technique of proton-spin contrast-variation improves the signal-to-noise ratio by more than one order of magnitude, thus enabling the direct determination of protonated tRNAs within a deuterated ribosome for the first time. Here we analyze a pair of ribosomal complexes being either in the pre- or post-translocational states that represent the main states of the elongating ribosome. Both complexes were derived from one preparation. The orientation of both tRNAs within the ribosome and their mutual arrangement are determined by using an electron microscopy model for the *Escherichia coli* ribosome and the tRNA structure. The mass center of gravity of the $(tRNA)_2$mRNA complex moves within the ribosome by 12 ± 4 Å in the course of translocation as previously reported. The main results of the present analysis are that the mutual arrangement of the two tRNAs does not change on translocation and that the angle between them is, depending on the model used, 110° ± 10° before and after translocation. The translocational movement of the constant tRNA complex within the ribosome can be described as a displacement toward the head of the 30S subunit combined with a rotational movement by about 18°.**

The central machinery of the translational apparatus is the ribosome, which is one of the most complicated cellular structures. It separates into two subunits and consists of more than 50 components. The central RNA ligands of the ribosome during protein synthesis are tRNAs and mRNA. mRNA brings the genetic information to the ribosome where tRNAs are used to interpret the codon sequence of the mRNA in terms of an amino acid sequence in the growing peptide (for a recent synopsis see ref. 1). Data derived from cross-linking studies, chemical protection, and fluorescence measurements have led to the proposal of conflicting models for the tRNA positions in the elongating ribosome (2–4) because of uncertainties in the spatial assignment of ribosomal components. Thus, additional information on the location of tRNAs by using direct physical methods is necessary to evaluate and refine the models. Positions of tRNAs within the ribosome deduced from electron microscopy (EM) have been proposed recently (5, 6). Neutron-scattering analysis has been applied for direct localization of the mass center of gravity for the $(tRNA)_2$mRNA complex present on the ribosome during elongation (7).

Here we describe the relative arrangement of the tRNAs before and after translocation as derived from the neutron-scattering data. The mutual arrangement of the tRNAs does not change on translocation from their pre- to their post-translocational positions, and the angle between them remains constant at 110° ± 10°.

MATERIALS AND METHODS

Preparation of Ribosomal Elongation Complexes. Ref. 7 contains a detailed description of sources, biochemical preparations, and the isolation and characterization of the ribosomal elongation complexes used as samples for neutron-scattering analysis as well as for the preparation of the samples for proton-spin contrast variation. The respective complexes contained the RNA ligands (mRNA and two tRNAs) protonated in a fully deuterated ribosomal matrix in D_2O milieu.

Scattering Experiment and Data Collection. The method of proton-spin contrast variation (8, 9) was used for analyzing pre-translocational (PRE) and post-translocational (POST) states with the instrument SANS-1 (GKSS, Germany; ref. 10). This technique exploits the dependence of the hydrogen-scattering length on the orientation of the proton spins relative to that of the scattered neutrons. By polarization of the spins the signal from protonated components can be selectively enhanced. The proton spin alignment in the sample reaching about 70% was achieved by dynamic nuclear spin polarization (7, 10). For stabilization of the spin alignment the sample is kept at temperatures below 0.2 K. Both elongation states were measured two times for 1 week each. The functional integrity of the particles is not affected by this treatment as shown previously (7, 9).

Data Analysis. The primary scattering data were processed according to ref. 7, yielding the three basic scattering functions of proton-spin contrast variation (UU, HH, and UH; ref. 9). The basic scattering functions describe the ribosomal matrix (mainly UU) and provide information about the label structure (mainly HH) and the position of the label with respect to the ribosome (mainly the cross-term UH). The information about the spatial correlation between the scatterers inherent in these functions is not directly accessible. Instead, it has to be extracted by a systematic iteration process whereby theoretical scattering curves are calculated from models to reach an optimal fit with the experimental data set. A 70S ribosome model derived from electron microscopy with a resolution of about 25 Å (11) was combined with a simplified model for the

The publication costs of this article were defrayed in part by page charge payment. This article must therefore be hereby marked "*advertisement*" in accordance with 18 U.S.C. §1734 solely to indicate this fact.

Abbreviations: PRE and POST states, pre- and post-translocational elongation state of the 70S ribosome, respectively.

†To whom reprint requests should be addressed. e-mail: nierhaus_kh@mpimg-berlin-dahlem.mpg.de.

two tRNAs based on the crystal structure of the yeast $tRNA^{Phe}$ (12, 13). Each tRNA is represented by four spheres, the long arm with the anticodon comprising three spheres, and the short arm with the amino acid stem comprising two spheres (both arms have a common sphere at the elbow region of the tRNA, see Fig. 2). Neither the single-stranded region of the CCA-end nor the mRNA was considered in the model. The fitting procedure was done by an iterative calculation computer program that allows 20 physical and biochemical parameters to be varied. Most important are those parameters that describe the relative orientation of the RNA ligands within the ribosome. For describing the location of the protonated $(tRNA)_2$mRNA complex within the ribosomal matrix, polar coordinates were used, where the radius vector (r, φ, θ) extends from the mass center of gravity of the ribosome to that of the protonated label. The length of the radius vector is given by r, and the direction is defined by the angles φ and θ. φ ranges from 0 to 360° and θ, from 0 to 180°. For fitting the arrangement of the tRNAs, five additional parameters were optimized: (*i*) The tRNAs were allowed to separate from each other; (*ii*) the angle between the tRNAs was varied; and (*iii–v*) the whole tRNA model was allowed to rotate by the three Eulerian angles. The quality of the fit is quantified by the root mean square deviation (Δ) between the experimental and calculated intensities (I_{exp} and I_{calc}; Eq. **1**). The parameter set giving the lowest deviation is taken as the best representation of the 70S–tRNA arrangement.

$$\Delta = \sqrt{1/N \sum_{i=1}^{N} \left[\frac{I_{\exp}(Q_i) - I_{calc}(Q_i)}{\sigma_i} \right]^2} \qquad [1]$$

where σ = standard deviation, $I(Q)$ = intensity, Q = momentum transfer, and N = number of data points of an intensity curve.

A minor correction of the above-mentioned structural parameters may be expected from the fact that the PRE and POST states were established for at least 80% of the ribosomes carrying Ac[^{14}C]Phe-tRNA, respectively. In all cases, the presence of particles belonging to a minority of less than 20% is expected to give rise to deviations, which are included in the indicated errors.

RESULTS

Ribosomal Elongation States. PRE and POST states were prepared from fully deuterated ribosomes and protonated RNA ligands. Site-specific tRNA binding was achieved with a heteropolymeric mRNA of 46 nt that contained two unique codons, AUG-UUC, in the middle (MF-mRNA, ref. 7). In a first step, $tRNA_f^{Met}$ was bound to the ribosomal P site, and subsequently the ribosomal A site was filled with Ac[^{14}C]Phe-tRNA, thus establishing the PRE state. After elongation factor (EF)-G-dependent translocation with half of the sample, both tRNAs reside in the P and E sites, respectively (POST state). Unbound ligands were removed by ultracentrifugation. The puromycin reaction revealed that for either preparation, the PRE and the POST states, respectively, were established for at least 80% of the ribosomes carrying an Ac[^{14}C]Phe-tRNA. The tRNA occupation amounted to 0.5 Ac[^{14}C]Phe-tRNA per ribosome for both states (i.e., 50% of the ribosomes carried the protonated RNA ligand complex; for details of analysis see ref. 7). One sample contained about 6,000 pmol of either elongation state and was analyzed by proton-spin contrast variation with the instrument SANS-1 in Geesthacht (10).

Data Analysis. After reduction the collected data were deconvoluted into the three basic scattering functions [UU], [UH], and [HH] for the PRE and the POST states. Fig. 1 shows the cross-term [UH] that can be measured with the highest precision and thus is most important for determination of the relative arrangement of protonated and deuterated parts of the sample (for more information see ref. 7). In a previous approach the mass centers of gravity of the protonated $(tRNA)_2$mRNA complexes within the deuterated ribosome were determined in both the PRE and the POST states (7). To gain a more detailed insight into the elongating ribosome a simple four-sphere model for the tRNA was introduced (Fig. 2). The model was duplicated to represent the two tRNAs bound to the elongating ribosome. No significant difference was observed between the calculated scattering curves of the full set of about 2 × 1,600 atoms of the tRNAs within the ribosomal model and that of the 2 × 4 sphere tRNA model. This indicates that the eight-sphere model is a suitable description of the tRNAs within the ribosome for data analysis purposes at the present resolution.

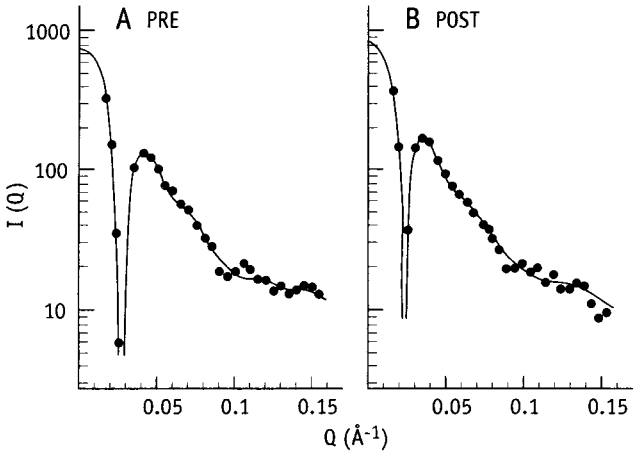

FIG. 1. The basic scattering functions [UH] for the pre- (*A*) and post-translocational (*B*) states (relative intensities versus the momentum transfer, *Q*). The cross-term [UH] can be measured with the highest precision from the three basic scattering functions (7), and thus gives the most solid information about the localization of the label within the 70S ribosome. The line indicates the fit to the experimental data points by using the 70S model of the Frank group (11) and the eight-sphere model of the tRNAs (Fig. 2).

The eight-sphere model of the tRNAs allowed positioning of its mass center within the ribosome model (7). Furthermore, it also can be used to extract the orientation of the tRNAs within the ribosome and the mutual arrangement of the two tRNAs for both states as shown in the following sections.

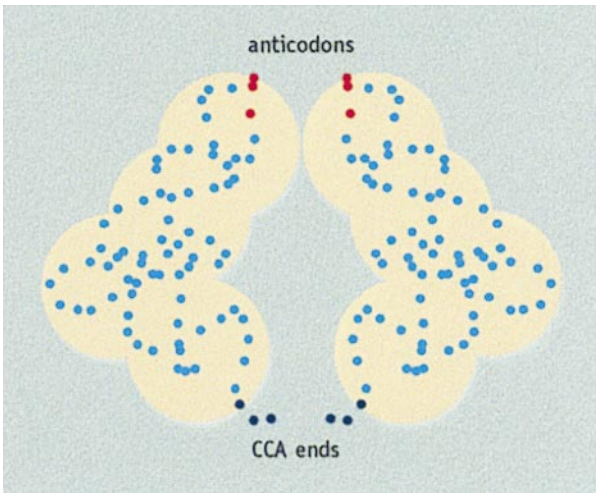

FIG. 2. Eight-sphere model of two tRNAs. The dots indicate the phosphorus atoms from the crystal structure of $tRNA^{Phe}$ (dark blue, CCA-3′ ends; red, anticodons; refs. 15 and 16). The tRNAs are shown in opposite arrangement (ψ = 180°).

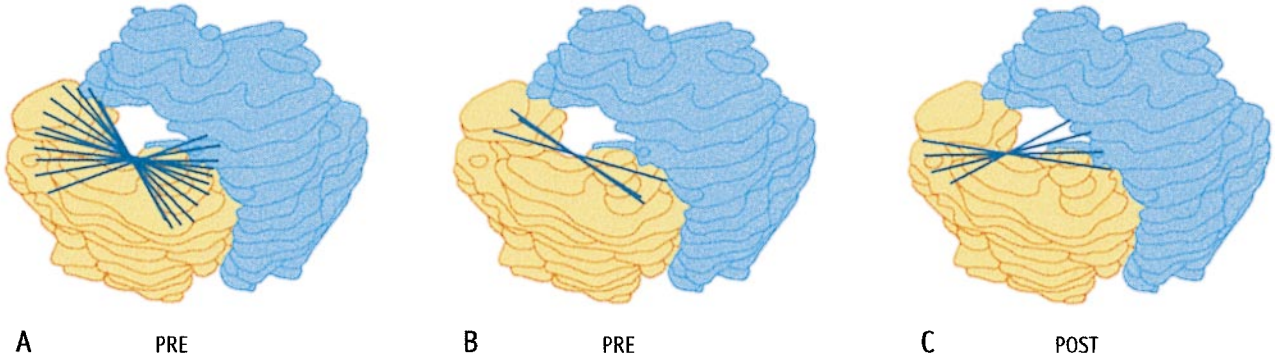

FIG. 3. Orientation of the tRNAs within the ribosome for the pre- (*A* and *B*) and the post- translocational (*C*) states. The orientations of the tRNAs are depicted by lines passing through the midpoint between the two anticodons and that between the two CCA ends. (*A*) Orientations with Δ values of 10% above the minimal deviation (1.479, calculated according to Eq. **1**). (*B* and *C*) Orientations with Δ values of 5% above the minimal deviation (1.479 and 1.334, respectively).

Orientation of the tRNAs Within the Ribosome. To elucidate the orientation of the tRNAs within the ribosome, the tRNAs were allowed to rotate around their optimized mass center during the fitting procedure. The general orientation of the tRNA can be illustrated by a line passing through the midpoint between the CCA-ends and that between the anticodons. In Fig. 3 *A* and *B* corresponding lines are drawn for all solutions for the PRE state with Δ values of up to 10% and up to 5% above the minimal deviation. An improved fit to the neutron-scattering data is accomplished with a clear tendency toward a more defined orientation, i.e., the data allow different orientations to be distinguished. A similar tendency was observed fitting the data of the POST state (Fig. 3*C*, all orientations with Δ values less than 5% above the minimal deviation, respectively).

Mutual Arrangement of both tRNAs. For fitting the mutual arrangement of the tRNAs, the eight-sphere model was further varied with respect to two parameters. First, the tRNAs were allowed to separate from each other, and second, the angle between the tRNAs was varied. During this processing step the tRNAs were still allowed to rotate around their mass center of gravity. In all solutions the tRNAs did not separate as would be expected for functional reasons at least in PRE states (see *Discussion*), thus giving credit to the results obtained. For the angle between the tRNAs (ψ) two minima were found for both the PRE and the POST states (Fig. 4*B*). ψ is defined in a way that $\psi = 0°$ indicates a parallel arrangement and $\psi = 180°$, an opposite arrangement of the tRNAs (Fig. 2). The plot of the deviation as a function of ψ (Fig. 4*B*) runs in parallel for PRE and POST states with the same location of minima at $\psi = 110° \pm 10°$ ($\Delta = 1.479$ for PRE and 1.334 for POST, respectively). The left half of Fig. 4*B* means the R configuration (i.e., the T side of the tRNA at the A position faces the D side of the tRNA at the P position; Fig. 4*A*) and the right half shows the mirror picture (S configuration; Fig. 4*C*). Because of the overall symmetry of the tRNA complexes in the R or S configuration our fitting procedure is not able to discriminate between these two possible general arrangements (2).

A sound model for the tRNA arrangement inside the ribosome has to consider the known location of the decoding process that takes place at the neck between the head and body of the 30S subunit (14–16) and that of the peptidyltransferase center at the root of the central protuberance toward the "L1" protuberance of the 50S subunit (17, 18). Assuming the R configuration, our model accommodates both anticodon tips of the tRNAs at the cleft of the 30S subunit with the CCA tips aiming at the 50S subunit below the central protuberance (Fig. 4*A*); in the S configuration the anticodon tips are at the same position but the CCA ends point downward toward the interface between the subunits. No direct conclusion can be drawn in favor of the R or the S configuration from the fitting procedure, because the minimal deviation was found to be identical in both the PRE and the POST states (Fig. 4*B*).

Fig. 5 summarizes the model for the tRNA arrangement in the elongating ribosome as derived from neutron scattering.

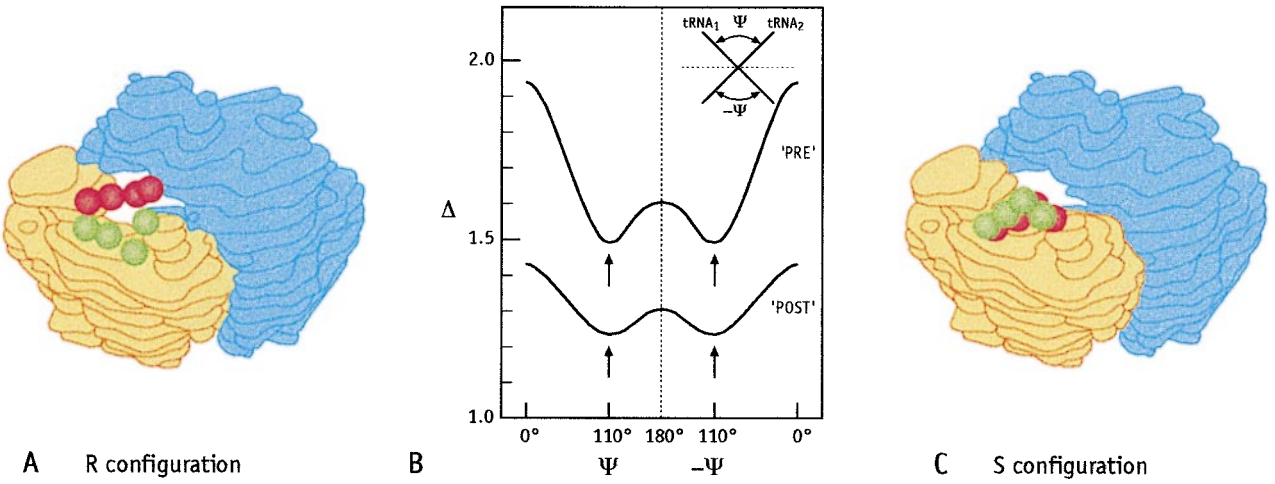

FIG. 4. Mutual arrangement of the tRNAs in the pre- and the post-translocational states. (*A*) Schematic representation of the R configuration in PRE by using the angle of 110°. (*B*) Dependence of the deviation Δ (Eq. **1**) on the angle ψ between both tRNAs. The left half represents the R configuration, and the right half represents the S configuration (see also *Insert*). The minimal deviation is found at angles of $\psi = 110° \pm 10°$. (*C*) Schematic representation of the S configuration in PRE by using the angle of 110°.

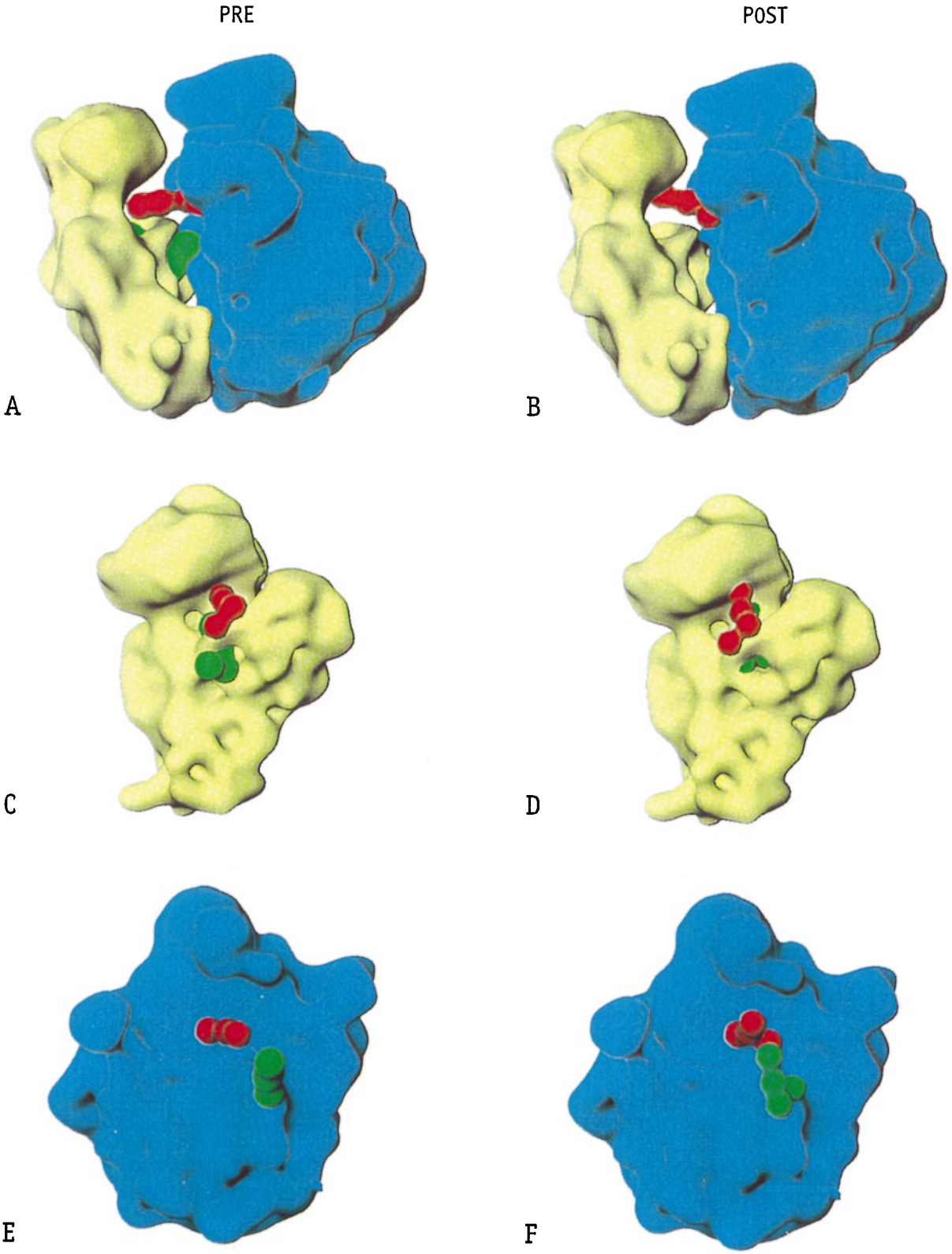

FIG. 5. tRNA arrangement in the PRE (*Left*) and POST states (*Right*). The green and red tRNAs are thought to be at the A and P sites, respectively, of PRE states and at the P and E sites, respectively, of POST states. Only the R configuration is shown. (*A* and *B*) 70S ribosome. (*C* and *D*) 30S subunit. (*E* and *F*) 50S subunit.

Because it is generally assumed that the ternary complex aminoacyl-tRNA·EF-Tu·GTP enters the A site next to the L7/L12 stalk (19), the green tRNA should be at the A site in PRE state (Fig. 5*A*, most easily seen in Fig. 5*E*). Accordingly, the red tRNA should be in the P site. It follows that after translocation the green tRNA should occupy the P site, and the red one should occupy the E site.

Fig. 5 *C* and *D* shows the tRNAs on the 30S interface viewed from the 50S subunit and Fig. 5 *E* and *F* shows the corresponding views on the 50S interface. The two tRNAs seem to

be separated by a thin bridge that is formed by the 30S subunit, and the tRNA at the P site in the POST state (green tRNA in Fig. 5*D*) seems to penetrate the surface of the 30S subunit by about 10 Å in depth. There are two possible reasons for this conflict. One reason might be the uncertainties of our measurements illustrated by the determination of the symmetry axis of the eight-sphere model of both tRNAs (Fig. 2) and by that of the angle between the tRNAs (Fig. 4). A second reason might be local conformational changes of the ribosome during the binding of the first tRNA. We note that the binding of the first tRNA to programmed ribosomes (P site) requires a high activation energy of 167 kJ mol^{-1} at 6 mM Mg^{2+}, indicating a conformational change of the ribosome (20).

The translocational movement may be deduced by comparing the tRNA positions in PRE and POST states. Because the mutual arrangement is the same before and after translocation, both tRNAs can be considered as one constant $(tRNA)_2$ complex that is displaced by about 12 ± 4 Å in the course of translocation mainly toward the head of the 30S subunit. This distance between the mass centers of the PRE and the POST states does not depend on the angle between tRNAs but is found invariantly to be 12 ± 4 Å (not shown). This lateral displacement is accompanied by a smooth rotational shift of about 18° ± 10° (Fig. 3; also compare Fig. 5 *C* and *D*).

DISCUSSION

Applying the new technique of proton-spin contrast variation, we recently reported the determination of the location of the mass center of the protonated $(tRNA)_2$mRNA complex within the elongating ribosome by neutron scattering (7). The results showed that (*i*) both tRNAs remained quantitatively bound during the translocation reaction and (*ii*) the mass center of gravity of the protonated complex moved by 12 ± 4 Å. Here we extend this analysis to the relative arrangement of the tRNAs in the elongating ribosome before and after translocation and propose a model for the arrangements of the tRNAs in both the PRE and the POST states (Fig. 5).

Our fitting approach by using an EM model of an empty ribosome with a resolution of about 25 Å (11) assumes that the shapes of empty ribosomes as well as of PRE and POST ribosomes are similar. This assumption is justified by a comparison of empty 70S ribosomes with those in the PRE and POST states by using x-rays and neutron-scattering techniques that revealed indistinguishable shapes within a resolution level of about 35 Å (21). In fact, in the present study the fit for both states of the elongating ribosome is of comparable quality when the same model for the ribosome is used (Fig. 1). A recent EM analysis also revealed no significant conformational change of 70S ribosomes in PRE and POST states (6).

Two observations in the present study are of pivotal importance for our understanding of the ribosomal elongation cycle. First, the mutual arrangement of the two tRNAs present on the ribosome in PRE and POST states does not change on translocation with an angle between the tRNAs of 110° ± 10° and neighbored acceptor stems as well as anticodon loops. At least in the PRE state both tips would be expected to be in proximity, because both anticodons are base-paired with adjacent mRNA codons (for review see ref. 22) and both CCA ends contact the peptidyltransferase center, thus fitting the representation in Fig. 2. The same representation was used for fitting the data of the POST state. The deviation values of the POST state are systematically lower than those of the PRE state (Fig. 4*B*), suggesting that the tRNA alignment shown in Fig. 2 is a valid description in both the PRE and the POST states.

An angle of about 100° ± 10° has been postulated for the R-configuration (23) according to both stereochemical considerations (24) and the effects of a mutational analysis of the anticodon loop of a tRNA (25), in good agreement with our results that yield an angle of 110°. We note, however, that in the stereochemical considerations (2), as well as in the present study, the crystal structure of the $tRNA^{Phe}$ was assumed to be present also on the ribosome, whereas a study of the accessibility of phosphate groups of tRNA revealed that tRNAs undergo conformational changes on binding to the ribosome (26), in agreement with a direct localization of three deacylated tRNAs by using electron cryomicroscopy (5). We further note that the use of a previous EM model of the ribosome from the Frank group also yielded a constant mutual arrangement of the tRNAs before and after translocation, but with an angle of 50° between the planes of the tRNAs, respectively. It follows that the mutual arrangement of the tRNAs does not change in the course of translocation is a model-invariant feature of the neutron-scattering results.

None of the conventional models of translocation requires a constant mutual arrangement of the tRNAs before and after translocation (for review see ref. 27) in contrast to a recently proposed model for the elongation cycle (28). This model was derived from an analysis of the contact patterns of tRNAs with ribosomal components at the various sites. It assumes the existence of a movable ribosomal carrier structure consisting of two tRNA binding regions (the so-called α- and ε-regions) that are present in A and P sites in the PRE state and in P and E sites in the POST state (α-ε model, ref. 28). The model predicts a stable mutual arrangement of both tRNAs bound to the carrier before, during, and after translocation.

tRNAs at A, P, and E sites contact the ribosomes over the whole structure from the anticodon loop to the aminoacyl stem (26, 28). It follows that the region that spans from the decoding center on the small subunit to the peptidyltransferase center on the large subunit along the tRNAs represents a "bridge" connecting the two subunits. An analysis of the bridges between the subunits within the 70S ribosome revealed six connective regions (see refs. 11, 29, and 30). Only one of these (bridge 2) is in the direct vicinity of the tRNAs. This most massive connection between both subunits might represent the movable α-ε carrier that transports both tRNAs tightly bound from the A and P sites to the P and E sites in the course of translocation.

The second observation is that the tRNAs that are bound to the P site are not in identical positions in the PRE and the POST states (Fig. 5). Thus, the P site does not represent a topographically fixed structure within the ribosome in contrast to the conventional view. Compatible results were obtained earlier in studies applying fluorescence energy transfer (31) and protection against chemical modification (32). According to the α-ε model the P site is not a topographically defined site but rather exists in different ribosomal regions depending on the functional state, namely the ε-region in the PRE state and the α-region in the POST state. Thus, the concept of a movable tRNA carrier suggested by the α-ε model convincingly reconciles the experimental evidence. Such a P site does not violate the classical definition, which refers to the puromycin reactivity of the P site-bound tRNA (33) rather than its topographical location.

Two EM localizations of the tRNAs within the ribosome were recently published (5, 6). There is agreement concerning the general location of the tRNAs within the ribosome between those studies and the results presented here. However, the results of the EM studies, although in conflict with each other, differ in one important aspect from the results presented here (for a detailed discussion see ref. 21). The images derived from the EM studies are interpreted in a way that the tRNA at the E site is dislocated at least at the anticodon region in a way that codon–anticodon interaction at the E site is excluded after translocation, whereas the neutron-scattering data argue for an *identical* mutual arrangement of the tRNAs before and after translocation, easily allowing codon–anticodon interaction at the E site. In contrast to both EM studies, a homologous

pair of PRE and POST states has been analyzed here for the first time. An EM study of an equivalent pair of authentic PRE and POST states is underway and might solve the discrepancies.

In summary, this study directly assesses the location, orientation, arrangement, and movement of the tRNAs in the elongating ribosome. An important outcome is that the mutual arrangement of the tRNAs does not change on translocation: The anticodon loops and CCA ends stay in close vicinity to each other, respectively.

We thank Drs. J. Frank and P. Penczek for discussions and for providing the 70S model, modeling the tRNAs within the ribosome, and making manuscripts available before publication. We are grateful to Drs. C. Trieber and C. M. T. Spahn for help and discussion. This work was supported by the Bundesministerium für Forschung und Technologie (03-NI 3 MPG), by the Deutsche Forschungsgemeinschaft (Ni174 8–1) and by the European Commission (CIPA CT 93–0158).

1. Matheson, A. T., Davies, J. A., Dennis, P. P. & Hill, W. E., eds. (1995) *Biochem. Cell Biol.* **73,** 739–1227.
2. Lim, V., Venclovas, C., Spirin, A., Brimacombe, R., Mitchell, P. & Muller, F. (1992) *Nucleic Acids Res.* **20,** 2627–2637.
3. Wower, J., Sylvers, L. A., Rosen, K. V., Hixson, S. S. & Zimmermann, R. A. (1993) in *The Translational Apparatus-Structure, Function, Regulation, Evolution*, eds. Nierhaus, K. H., Franceschi, F., Subramanian, A., Erdmann, V. & Wittmann-Liebold, B. (Plenum, New York), pp. 455–464.
4. Brimacombe, R. (1995) *Eur. J. Biochem.* **230,** 365–383.
5. Agrawal, R. K., Penczek, P., Grassucci, R. A., Li, Y., Leith, A., Nierhaus, K. H. & Frank, J. (1996) *Science* **271,** 1000–1002.
6. Stark, H., Orlova, E. V., Rinke-Appel, J., Jünke, N., Mueller, F., Rodnina, M., Wintermeyer, W., Brimacombe, R. & van Heel, M. (1997) *Cell* **88,** 19–28.
7. Wadzack, J., Burkhardt, N., Jünemann, R., Diedrich, G., Nierhaus, K. H., Frank, J., Penczek, P., Meerwinck, W., Schmitt, M., Willumeit, R. & Stuhrmann, H. B. (1997) *J. Mol. Biol.* **266,** 343–356.
8. Knop, W., Hirai, M., Olah, G., Meerwinck, W., Schink, H.-J., Stuhrmann, H. B., Wagner, R., Wenkow-EsSouni, M., Zhao, J., Schärpf, O., Crichton, R. R., Krumpolc, M., Nierhaus, K. H., Niinikoski, T. O. & Rijllart, A. (1991) *Physica B* **174,** 275–290.
9. Stuhrmann, H. B., Burkhardt, N., Diedrich, G., Jünemann, R., Meerwinck, W., Schmitt, M., Wadzack, J., Willumeit, R., Zhao, J. & Nierhaus, K. H. (1995) *Nuclear Instr. Methods* **A 356,** 124–132.
10. Zhao, J., Meerwinck, W., Niinikoski, T., Rijllart, A., Schmitt, M., Willumeit, R. & Stuhrmann, H. B. (1995) *Nuclear Instr. Methods* **A 356,** 133–137.
11. Frank, J., Zhu, J., Penczek, P., Li, Y., Srivastava, S., Verschoor, A., Radermacher, M., Grassucci, R., Lata, T. K. & Agrawal, R. K. (1995) *Nature (London)* **376,** 441–444.
12. Kim, S. H., Quigley, G. J., Suddath, F. L., McPherson, A., Sussman, J. L., Wang, A. H. J., Seeman, N. C. & Rich, A. (1974) *Science* **185,** 435–440.
13. Robertus, J. D., Ladner, J. E., Finch, L. T., Rhodes, D., Brown, R. S., Clark, B. F. C. & Klug, A. (1974) *Nature (London)* **250,** 546–551.
14. Shatsky, I. N., Mochalova, L. V., Kojouharova, M. S., Bogdanov, A. A. & Vasiliev, V. D. (1979) *J. Mol. Biol.* **133,** 501–515.
15. Gornicki, P., Nurse, K., Heilmann, W. Boublik, M. & Ofengand, J. (1984) *J. Biol. Chem.* **259,** 10493–10498.
16. Olson, H. M., Lasater, L. S., Cann, P. A. & Glitz, D. G. (1988) *J. Biol. Chem.* **263,** 15196–15204.
17. Wower, J., Hixson, S. S. & Zimmermann, R. A. (1989) *Proc. Natl. Acad. Sci. USA* **86,** 5232–5236.
18. Cooperman, B. S., Weitzmann, C. J. & Fernández, C. L. (1990) in *The Ribosome: Structure, Function, and Evolution*, eds. Hill, W. E., Dahlberg, A., Garrett, R. A., Moore, P. B., Schlesinger, D. & Warner, J. R. (Am. Soc. Microbiol., Washington, DC), pp. 491–501.
19. Stöffler, G. & Stöffler-Meilicke, M. (1986) in *Structure, Function, and Genetics of Ribosomes*, eds. Hardesty, B. & Kramer, G. (Springer, New York), pp. 28–46.
20. Schilling-Bartetzko, S., Bartetzko, A. & Nierhaus, K. H. (1992) *J. Biol. Chem.* **267,** 4703–4712.
21. Nierhaus, K. H., Stuhrmann, H. B. & Svergun, D. (1998) *Prog. Nucleic Acids Res. Mol. Biol.* **59,** in press.
22. Nierhaus, K. H. (1990) *Biochemistry* **29,** 4997–5008.
23. Lim, V. I. (1997) *J. Mol. Biol.* **266,** 877–890.
24. Lim, V. I. & Venclovas, C. (1992) *FEBS Lett.* **313,** 133–137.
25. Smith, D. & Yarus, M. (1989) *Proc. Natl. Acad. Sci. USA* **86,** 4397–4401.
26. Dabrowski, M., Spahn, C. M. T. & Nierhaus, K. H. (1995) *EMBO J.* **14,** 4872–4882.
27. Nierhaus, K. H. (1996) in *GroupI Introns and Ribosomal RNA*, eds. Green, R. & Schroeder, R. (Landes Company, Austin), pp. 69–81.
28. Nierhaus, K. H., Beyer, D., Dabrowski, M., Schäfer, M. A., Spahn, C. M. T., Wadzack, J., Bittner, J.-U., Burkhardt, N., Diedrich, G., Jünemann, R., Kamp, D., Voss, H. & Stuhrmannm, H. B. (1995) *Biochem. Cell Biol.* **73,** 1011–1021.
29. Frank, J., Verschoor, A., Li, Y., Zhu, J., Lata, R. K., Radermacher, M., Penczek, P., Grassucci, R., Agrawal, R. K. & Srivastava, S. (1995) *Biochem. Cell Biol.* **73,** 757–765.
30. Lata, K. R., Agrawal, R. K., Penczek, P., Grassucci, R., Zhu, J. & Frank, J. (1996) *J. Mol. Biol.* **262,** 43–52.
31. Hardesty, B., Odom, O. W. & Deng, H.-Y. (1986) in *Structure, Function, and Genetics of Ribosomes*, eds. Hardesty, B. & Kramer, G. (Springer, New York), pp. 47–67.
32. Moazed, D. & Noller, H. F. (1989) *Nature (London)* **342,** 142–148.
33. Traut, R. R. & Monro, R. E. (1964) *J. Mol. Biol.* **10,** 63–72.